Hindawi
International Journal of Antennas and Propagation
Volume 2022, Article ID 6486628, 6 pages
https://doi.org/10.1155/2022/6486628

Research Article

Design of a W-Band Dielectric Phase Shifter Based on Liquid Crystal

Wei Hu,[1] Di Jiang,[1] Weiyi Zhang,[1] Yuxin Liu,[1] Kai Zhu ,[1] and Tiedi Zhang[2]

[1]*Information and Communication Engineering, University of Electronic Science and Technology of China, Chengdu 611731, China*
[2]*Electronic Science and Engineering, University of Electronic Science and Technology of China, Chengdu 611731, China*

Correspondence should be addressed to Kai Zhu; zhukai1278@163.com

Received 21 May 2022; Revised 27 September 2022; Accepted 17 October 2022; Published 15 November 2022

Academic Editor: Mauro Parise

Copyright © 2022 Wei Hu et al. This is an open access article distributed under the Creative Commons Attribution License, which permits unrestricted use, distribution, and reproduction in any medium, provided the original work is properly cited.

In this paper, a W band (75–110 GHz) phase shifter based on the liquid crystal of continuous tunability and the three-electrode bias network of excellent electrical manipulation is designed. Taking Rexolite 1422 as the transmission dielectric, in which slots are dug and filled with liquid crystal. The voltage is regulated by the electrode bias network, and then the liquid crystal dielectric constant is changed to realize phase shift. The measured results show that the phase shift of the liquid crystal dielectric phase shifter can be up to 440° through the electrical control of the bias electrode network, which surpasses many designed phase shifters. In the whole W band, the insert loss is about 3 dB and the return loss is almost over 10 dB, emerging excellent matching.

1. Introduction

With the development of high-resolution imaging radar and broadband wireless communication, the demand for high-frequency controllers is increasing and much more scholars are devoted to the research of phase shift structure, which has the advantages of large instantaneous bandwidth and high resolution. With higher frequency, the main obstacle to overcome is high path loss [1]. The high gain antenna can better compensate for the path loss by transmitting the directional beam point to point [2], which requires beam deflection to offset the spatial misalignment or to track the mobile terminal. A phased array antenna can guide its main beam by providing different phase shifts to each antenna element. The phase difference is supplied by a tunable phase shifter, whose phase shift can be dynamically regulated in the light of the expected phase distribution of the antenna element. However, the realization of broadband and low-loss beam steering at high frequency is still challenging, mainly due to the lack of practical phase shifters [3].

At the moment, there are two major tendencies in the development of phase shifters. One is to explore new special materials and utilize the variety of material properties to cause the change of phase constant, thus leading to phase shift, such as liquid crystal (LC) phase shifter [4] and graphene phase shifter [5]. The other is the phase shifter based on a microelectromechanical system (MEMS) [6] and a monolithic microwave integrated circuit (MMIC) [7]. Liquid crystal composed of anisotropic molecules is considered to be one of the optimal materials for tunable devices due to its excellent ability of tunable permittivity and wide tuning range. The anisotropy of liquid crystal enables the quasi-static electrostatic field to alter the value of the dielectric constant between two extreme states, so as to realize the phase controllability [8]. Moreover, the devices based on liquid crystal have many apparent advantages, such as small volume, lightweight, low cost, simple process, and continuous adjustment.

The W band (75–110 GHz) liquid crystal phase shifter in [9] achieved a high Figure of Merit (FoM) of about 135°/dB, yet limited to magnetic bias. In [10, 11], two designs of W-band liquid crystal phase shifters achieved better results. In [12], an electrode system of W- and LC phase shifters was proposed but only verified in simulation.

This paper applies Rexolite 1422 (a unique crosslinked polystyrene microwave plastic with a dielectric constant of

2.53, and a loss tangent of about 0.002) in processing the liquid crystal dielectric phase shifter, which greatly reduces the cost of the phase shifter. And the liquid crystal material in this paper is VMLC2101, with relative permittivity from $\varepsilon_{r,\perp} = 2.35$ to $\varepsilon_{r,\parallel} = 3.21$ and loss tangent from $\tan\delta_{\perp} = 0.0096$ to $\tan\delta_{\parallel} = 0.0053$. The three-electrode bias network is designed to regulate the dielectric constant of liquid crystals. Meanwhile, the wonderful dielectric performance of the designed liquid crystal dielectric phase shifter in the W band appears. Comparing the test with the simulation, it can be seen that the electromagnetic wave conduction with low power consumption and low loss is successfully realized.

2. Design of Phase Shifter

2.1. Theory. Since liquid crystal molecules can be continuously oriented, the phase shifters are also continuously tunable. The maximum differential phase shift of the liquid crystal phase shifter is computed as

$$\Delta\phi = l \cdot \left(\Delta\beta \cdot \frac{180^{\circ}}{\pi}\right) = l \cdot \left(\left(\sqrt{\varepsilon_{\parallel}} - \sqrt{\varepsilon_{\perp}}\right) \cdot \frac{360^{\circ} \cdot f}{c_0}\right), \quad (1)$$

where l is the phase shift length, $\Delta\beta = \beta_{\parallel} - \beta_{\perp}$ is the differential phase constant, besides, $\varepsilon_{\parallel}$ and $\varepsilon_{\perp}$ are the permittivity of liquid crystals in parallel and perpendicular directions, respectively. To compare these phase shifters, the following two parameters are considered in [13]. First, the steering efficiency is defined as

$$\tau_{\phi} = \frac{\Delta\phi}{l}, \quad (2)$$

which defines the differential phase shift per unit length, which is considered if a compact phase shifter is needed. Second, the FoM is defined as

$$\text{FoM} = \frac{\Delta\phi}{IL}, \quad (3)$$

where IL is the insertion loss for all tuning states. This paper will use the parameter to analyze and compare the designed phase shifter in the part III.

We measured the permittivity and loss tangent of the liquid crystal used in our experiment by terahertz time-domain spectroscopy (TDS) [14], and the results are shown in Figures 1 and 2. At the beginning of the voltage increase, the curve changes slowly because there is a threshold voltage for the deflection of liquid crystal molecules, that is, the deflection starts slowly after reaching this voltage. When the voltage is 350 V, the maximum variation is due to the remarkable deflection effect of liquid crystal molecules under the continuous influence of the electric field. When the voltage increases by 400 V, the dielectric constant and loss tangent tend to be stable. Therefore, we can realize the tuning of liquid crystal by applying 400 V voltage to the electrode in the experiment.

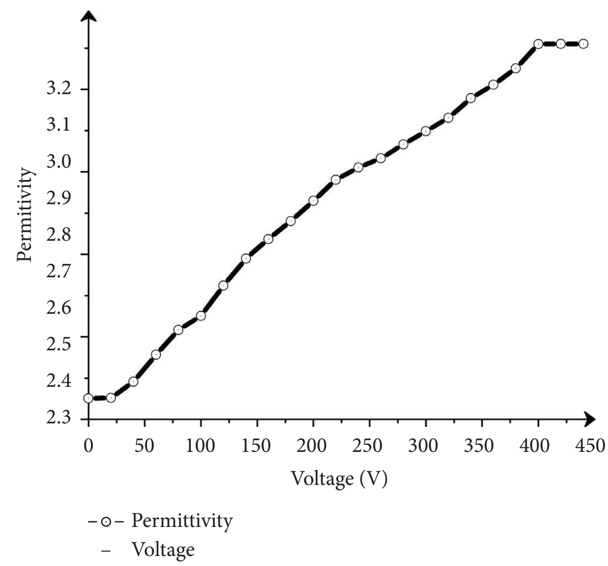

FIGURE 1: The permittivity of liquid crystal versus bias voltage.

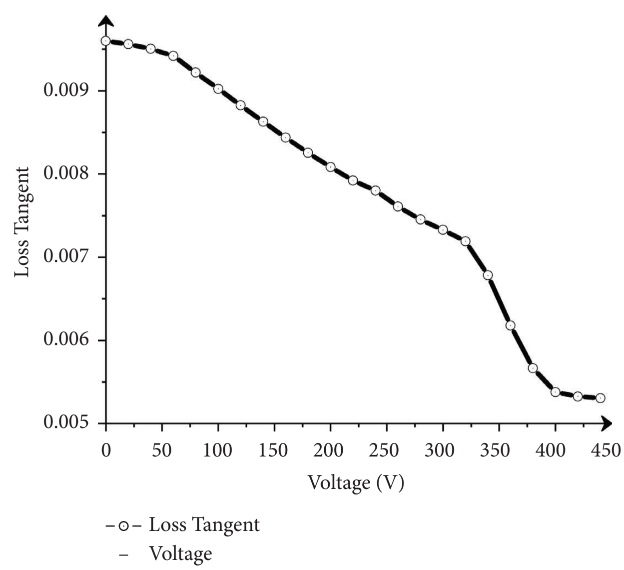

FIGURE 2: The loss tangent of liquid crystal versus bias voltage.

2.2. Bias Electrode Network. For the orientation of the liquid crystal, an external bias field is indispensable. Whether it is electric or magnetic, the liquid crystal molecules will be aligned along the loaded bias field. However, magnetic bias devices are relatively large and bulky, have high power consumption, and are difficult to integrate. Electronic bias can overcome the above problems, but an additional voltage bias network is essential, which will affect the propagation of the electromagnetic wave. The objective of the liquid crystal bias field is to set up a controllable electric field to realize the deflection of liquid crystal molecules, so as to change the dielectric constant of liquid crystal. On the one hand, it is necessary to ensure that the bias field applied by voltage can be accurately controlled. On the other hand, the interference with the electromagnetic wave across the bias field should be minimized.

According to the aforementioned bias field requirements, three pairs of electrodes are employed to attain parallel and orthogonal electric fields. The schematic

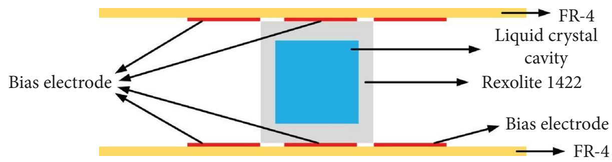

Figure 3: The schematic diagram of the dielectric phase shifter.

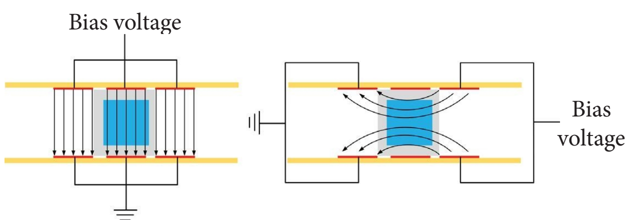

Figure 4: The electric field distribution diagram.

diagram of the liquid crystal dielectric phase shifter is shown in Figure 3. Three pairs of electrodes are etched on the inner side of the FR-4 substrate. The core of the phase shifter is the Rexolite dielectric strip with the liquid crystal in the center.

The electric field distribution diagram of the liquid crystal dielectric phase shifter is shown in Figure 4. When the upper electrodes are applied with positive voltage and the lower electrodes are grounded, an orthogonal electric field is formed between the substrates, and the dielectric constant of the liquid crystal is $\varepsilon_{\perp}$. When the middle electrodes are not electrified, one pair of slotted elliptical electrodes are applied with a positive voltage, and the other pair of slotted elliptical electrodes are grounded, a parallel electric field is formed between the substrates, and the dielectric constant of the liquid crystal is $\varepsilon_{\parallel}$. Through the variation of voltage value in the above two states, the dielectric constant of the liquid crystal can be continuously adjusted, and then the excellent phase shift characteristic can be achieved. In addition, the distribution of the latter electric field is not uniform, so it cannot guarantee that all liquid crystal molecules can be completely deflected, meaning that the dielectric constant of the liquid crystal cannot reach $\varepsilon_{\parallel}$.

The bias electrode network is designed by combining the structure of stub line, slotting, and ellipse, as presented in Figure 5. Since the electrodes are placed on Rexolite dielectric, the electromagnetic wave will be coupled to the bias electrodes, leading to frequency resonance and RF leakage, which seriously affect the transmission efficiency. Therefore, the impacts on RF propagation modes must be minimized. As for a simple straight bias line, the parasitic effect will be excited. To avoid this drawback, a mode suppression electrode structure is designed. Through simulation analysis, all electrodes are slotted to suppress frequency resonance and minimize the impact on high-frequency electromagnetic waves transmitted. In addition, the stub is designed to avoid RF leakage of the DC power feeder. The bonding pad on the substrate is connected with an external voltage source by using a low-frequency connection line to provide bias voltage. The screws fix the electrode network through the screw holes at the diagonal end of the substrate.

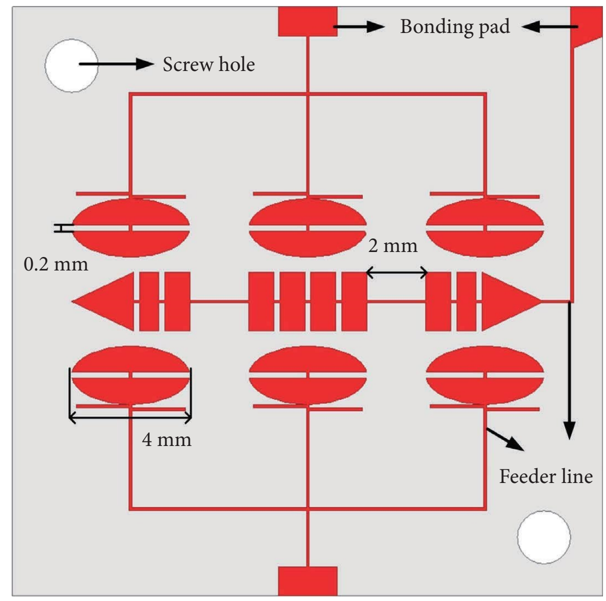

Figure 5: The bias electrode network.

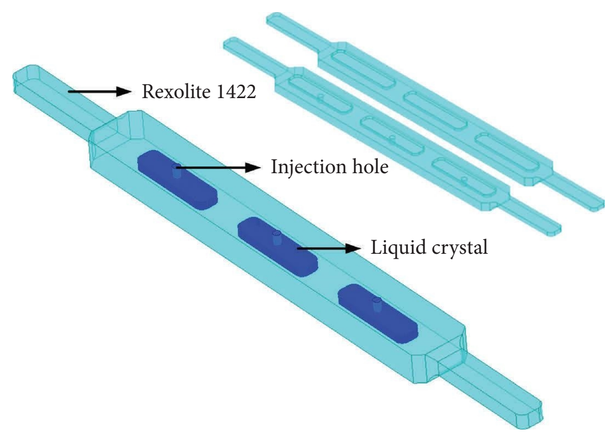

Figure 6: The Rexolite dielectric strip.

Rexolite 1422 is placed in the middle of the FR-4 substrates as the dielectric material, and each end of the dielectric strip extends into the WR-10 transition waveguide to reduce the wave transmission loss at the node. The dielectric strip is shown in Figure 6, for avoiding air bubbles when pouring liquid crystal, the liquid crystal groove is divided into three, and the three evenly spaced grooves are filled with the liquid crystal in the injection hole. Considering the need to excavate the liquid crystal grooves and injection holes in the actual processing, Eexolite dielectric strip is divided into two halves for excavation and then bonded.

2.3. Fabrication. The configuration of the dielectric phase shifter based on liquid crystal is shown in Figure 7, including two half blocks of Rexolite dielectric strips and a bias electrode network. Rexolite dielectric strips are bonded with plastic adhesive and dried. The metal electrode patches of the bias electrode network are horizontally etched on the FR-4 substrates.

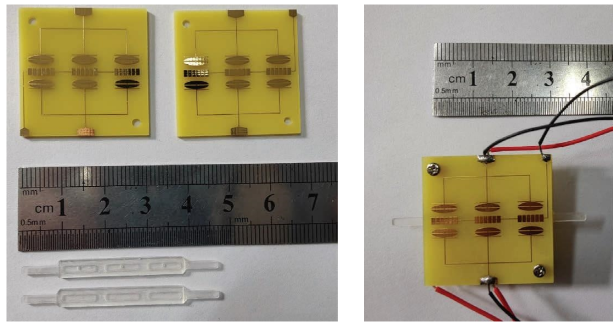

(a) (b)

Figure 7: The configuration of the phase shifter: (a) components and (b) whole.

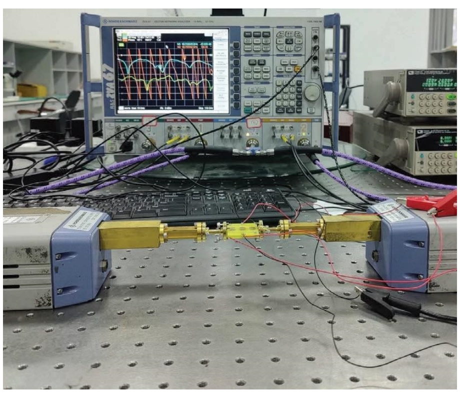

Figure 8: The test diagram of the phase shifter.

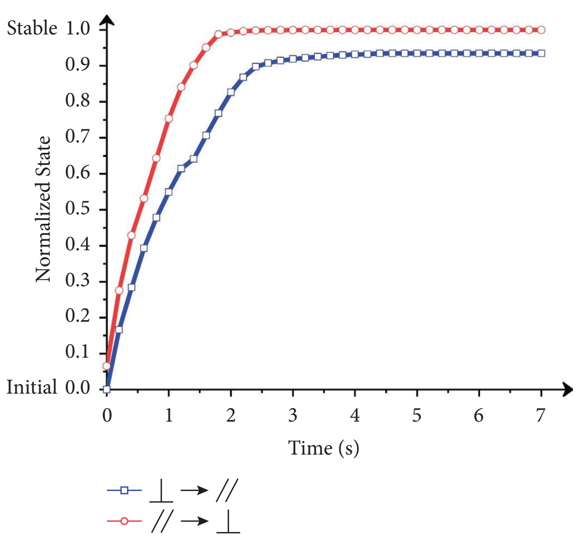

Figure 9: The state curve from initial to stable.

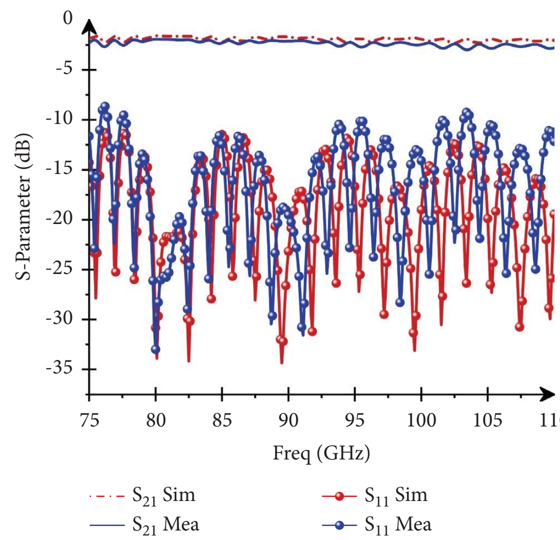

Figure 10: The results of the reflection coefficient.

3. Simulation and Measurement Results

The test diagram is shown in Figure 8, where the two WR-10 transmission waveguides sequentially connected with the frequency converter ZVA-Z110E and the vector network analyzer ZVA67 lie at both ends, and the liquid crystal dielectric phase shifter with an external voltage of 400 V to the bias electrode is seated in the middle. The electromagnetic wave is transmitted and received through the WR-10 transition waveguide, and the phase shift is realized through the intermediate phase shifter.

For the switching time, we plotted the normalized state curve from initial to stable shown in Figure 9 based on the results of the experiments. The time from parallel to perpendicular orientation is about 4.4 s, and it only takes about 2.4 s from perpendicular to parallel orientation. It is worth noting that since the perpendicular electric field (left in Figure 4) is more uniformly distributed than the parallel electric field (right in Figure 4), the excited electric field is more straightforward, so the perpendicular to parallel switching is faster.

In the W band range, the simulation and measurement results of the reflection coefficient are plotted in Figure 10. It can be seen that the reflection coefficient $|S_{11}|$ is almost over 10 dB, and the insertion loss is less than −3.5 dB, proving excellent matching. The phase shift and the FoM at 98 GHz are drawn in Figure 11. The maximum phase shift is equal to 440°, and the FoM nearly exceeds 140°/dB. The comparison between previous works in phase shifters based on a liquid crystal and this work is listed in Table 1. It can be informed that the dielectric phase shifter based on liquid crystal

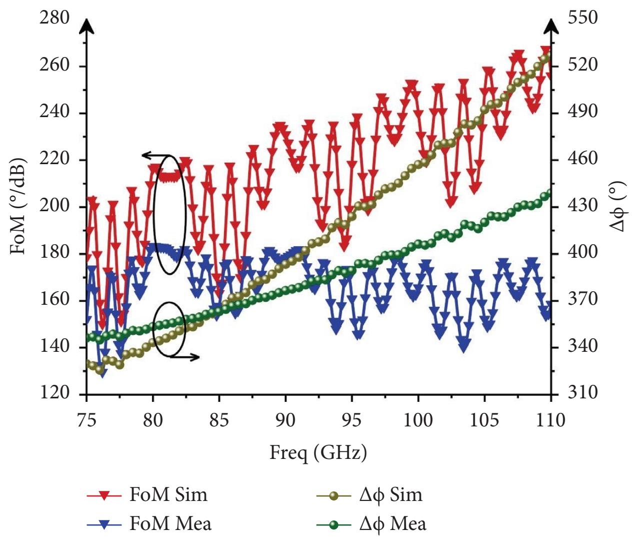

Figure 11: The results of phase shift and FoM.

Table 1: Comparison of previous works with this work.

Ref.	Band (GHz)	Max phase shift (°)	Max FoM (°/dB)	Note
[9]	99–105	307–318	135	Limited to magnetic bias
[10]	75–110	320–605	78	—
[11]	75–106	220–430	100	—
[12]	96–104	364–384	115	Limited to simulation
[15]	75–110	400–900	145	—
This work	75–110	340–440	182	—

achieves outstanding phase shift characteristics in the frequency band of nearly 100 GHz.

4. Conclusion

In this paper, the phase shifter using liquid crystal material realizes the compact design of the liquid crystal dielectric phase shifter and bias electrode network. It tremendously reduces the cost of the phase shifter, assures the steady dielectric performance of the liquid crystal phase shifter in a high-frequency band, and has low power consumption and low loss conduction of electromagnetic waves.

Data Availability

Data are available upon request.

Conflicts of Interest

Drs. Tianming Bai Tianliang Zhang Jie Gao and Kainan Qi (https://ieeexplore.ieee.org/document/9569888/authors#authors) are not included in this manuscript. The above four authors have only participated in the initial work of the published conference article (https://ieeexplore.ieee.org/document/9569888). The authors have obtained the consent of the above four authors for not adding them as authors in this manuscript. All authors in this paper disclosed no relevant relationships.

Acknowledgments

This work was supported by the National Natural Science Foundation of China (Grant No.61871086); the Science and Technology Support Project of Sichuan Province (2022YFG0015, 2022YFG0004); Sichuan Province Outstanding Young Science and Technology Talent Project (2021JDJQ0026); Central University Fund (ZYGX2019J007); and Funding of GF Science and Technology Key Laboratory (612502200303). The authors would like to thank the 2021 14th UK-Europe China Workshop on Millimetre-Waves and Terahertz Technologies (UCMMT) for its recognition of the preliminary work (https://ieeexplore.ieee.org/document/9569888).

References

[1] C. Han, A. O. Bicen, and I. F. Akyildiz, "Multi-wideband waveform design for distance-adaptive wireless communications in the terahertz band," *IEEE Transactions on Signal Processing*, vol. 64, no. 4, pp. 1–922, 2015.

[2] J. F. Du, D. Chizhik, and R. A. Valenzuela, G. Castro, M. Rodriguez, T. Chen, M. Kohli, and G. Zussman, Directional measurements in urban street canyons from macro rooftop sites at 28 GHz for 90% outdoor coverage," *IEEE Transactions on Antennas and Propagation*, vol. 69, no. 6, pp. 3459–3469, 2021.

[3] H. Liang, H. Zeng, Y. Zhang, and Z. Yang, "Broadband linear phase shifting of terahertz wave with low insertion loss by artificial-microstructure phase manipulation chip," in

Proceedings of the 2020 IEEE MTT-S International Microwave Workshop Series on Advanced Materials and Processes for RF and THz Applications (IMWS-AMP), pp. 1–4, Suzhou, China, July 2020.

[4] D. C. Zografopoulos, A. Ferraro, and R. Beccherelli, “Liquid-crystal high-frequency microwave Technology: materials and characterization,” *Advanced Materials Technologies*, vol. 4, no. 2, Article ID 1800447, 2018.

[5] G. He, G. Shkerdin, and J. Stiens, “Phase modulation properties of rectangular metallic waveguide with graphene integrated in sub-terahertz wave frequency range,” in *Proceedings of the IEEE Mtt-s International Microwave Workshop Series on Advanced Materials & Processes for Rf & Thz Applications*, July 2016.

[6] U. Shah, E. Decrossas, C. Jung-Kubiak, I. Mehdi, and J. Oberhammer, “Submillimeter-wave 3.3-bit RF MEMS phase shifter integrated in micromachined waveguide,” *IEEE Transactions on Terahertz Science and Technology*, vol. 6, no. 5, pp. 1–10, 2016.

[7] D. M. Zaiden, J. E. Grandfield, and T. M. Weller, “Compact and wideband MMIC phase shifters using tunable active inductor-loaded all-pass networks,” *IEEE Transactions on Microwave Theory and Techniques*, vol. 66, no. 2, pp. 1047–1057, 2018.

[8] A. G. Dyadyusha, T. Y. Marusii, and Y. A. Reznikov, “Orientational effect due to a change in the anisotropy of the interaction between a liquid crystal and a bounding surface,” *JETP Letters*, vol. 56, no. 1, pp. 17–21, 1992.

[9] M. Jost, C. Weickhmann, and S. Strunck, “Liquid crystal based low-loss phase shifter for W-band frequencies,” *Electronics Letters*, vol. 49, no. 23, pp. 1460–1462, 2013.

[10] S. Mueller, F. Goelden, P. Scheele, M. Wittek, C. Hock, and R. Jakoby, “Passive phase shifter for W-band Applications using liquid crystals,” in *Proceedings of the 2006 European Microwave Conference*, pp. 306–309, Manchester, UK, September 2006.

[11] R. Reese, M. Jost, H. Maune, and R. Jakoby, “Design of a continuously tunable W-band phase shifter in dielectric waveguide topology,” in *Proceedings of the 2017 IEEE MTT-S International Microwave Symposium (IMS)*, pp. 180–183, Hawaii, HI, USA, June 2017.

[12] M. Jost, C. Weickhmann, S. Strunck et al., “Electrically biased W-band phase shifter based on liquid crystal,” in *Proceedings of the International Conference on Infrared, Millimeter, and Terahertz waves (IRMMW-THz)*, pp. 14–19, Tucson, AZ, USA, September 2014.

[13] E. Polat, H. Tesmer, R. Reese, P. Schumacher, R. Jakoby, and H. Maune, “Reconfigurable millimeter-wave components based on liquid crystal Technology for smart applications,” *Crystals*, vol. 10, no. 5, pp. 346–351, 2020.

[14] M. Naftaly, N. Shoaib, and D. Stokes, “Intercomparison of terahertz dielectric measurements using vector network analyzer and time-domain spectrometer,” *Journal of Infrared, Millimeter and Terahertz Waves*, vol. 37, no. 7, pp. 691–702, 2016.

[15] R. Reese, E. Polat, H. Tesmer et al., “Liquid crystal based dielectric waveguide phase shifters for phased arrays at W-band,” *IEEE Access*, vol. 7, Article ID 127032, 2019.